Analytical Expression for Measurement of Intrinsic Coupling Loss in Multistep Index Optical Fibers

G. Aldabaldetreku, G. Durana, J. Zubia, and J. Arrue

***Abstract*—The aim of this paper is to obtain an analytical expression for intrinsic coupling losses in multistep index (MSI) fibers. For this purpose, a uniform power distribution is assumed. In order to validate the theoretical expression, the obtained results were compared with computer simulations using the ray-tracing method as well as with results obtained using existing models for step index (SI) and clad power-law profile graded index (GI) fibers. This analytical expression will provide fiber manufacturers with a very valuable tool for the assessment of fiber quality in terms of waveguide tolerances.**

***Index Terms*—Geometric optics, intrinsic coupling loss, MSI optical fibers, polymer optical fibers.**

I. Introduction

MULTISTEP index (MSI) fibers, and especially MSI polymer optical fibers (MSI-POFs), are currently being investigated because of their potential capabilities of achieving the high bandwidths of their graded index (GI) counterparts, namely, GI-POFs [1]–[5]. Their good performance is due to the better stability of their refractive index profiles with aging, and temperature and humidity fluctuations in comparison with GI fibers, thus increasing their popularity.

In another paper [6], we investigated the effects on the intrinsic coupling loss of the inevitable variations in waveguide properties as a result of standard manufacturing processes. Additionally, we have identified the most critical parameters, which are, namely, the numerical aperture and the core diameter. Simulations were performed using the ray-tracing method, which are much more realistic and include more effects susceptible to cause further losses. Even so, it would still be interesting to have a compact analytical expression, especially one involving the most influential parameters and simple enough to be implemented even in any programmable pocket calculator. This expression would allow manufacturers to easily obtain an accurate estimation of the incurred intrinsic coupling loss for any given tolerance in MSI fibers.

The structure of the paper is as follows. First of all, we derive a theoretical expression for MSI fibers that allows us to evaluate each intrinsic coupling loss mechanism separately, and then we compare this expression with formulae available for step index (SI) and GI fibers. This task is carried out by running a set of computer simulations, which involve joining two fibers randomly chosen from a given population following a normal distribution [7], [8]. Afterward, we carry out several simulations with appropriate waveguide variations for SI, GI, and three different MSI fibers using the ray-tracing method in an attempt to validate the theoretical results obtained before. Finally, we summarize the main conclusions.

Manuscript received July 8, 2005; revised October 27, 2005. This work was supported by the Universidad del País Vasco-Euskal Herriko Unibertsitatea and the Ministerio de Ciencia y Tecnología under Project 9/UPV 00147.345-14626/2002ZUBIA and Project TIC2003-08361.

The authors are with the Department of Electronics and Telecommunications, ETSI de Bilbao, University of the Basque Country, E-48013 Bilbao, Spain (e-mail: gotzon.aldabaldetreku@ehu.es).

Digital Object Identifier 10.1109/JLT.2005.863282

II. Derivation of an Analytical Expression for MSI Fibers

MSI fibers are structurally very similar to their SI or GI counterparts, since they consist of a core, a cladding that surrounds the core, and a protective jacket covering the cladding. The main difference is that the core consists of several layers of different refractive indices. The most general refractive index profile in MSI fibers can be expressed as

$$n(r) = \begin{cases} n_1, & r < \rho_1 \\ n_2, & \rho_1 \leqslant r < \rho_2 \\ \vdots & \\ n_N, & \rho_{N-1} \leqslant r < \rho_N \\ n_{cl}, & r \geqslant \rho_N \end{cases}. \tag{1}$$

For the sake of simplicity, we will neglect the possible effects of the protective jacket and assume that the cladding extends to infinity.

Our starting point is the calculation of the amount of source power carried by bound rays P_{br}. As stated in [9], for a diffuse or Lambertian light source of intensity $I_0 \cos\theta_0$ and an MSI fiber of N layers, P_{br} is given as a function of the total mode volume V by

$$P_{br} = \frac{I_0}{n_0^2} V, \qquad V = 2\pi^2 \int_0^{\rho_N} r S(r)\, dr \tag{2}$$

and taking into account that $S(r) = n_i^2 - n_{cl}^2 = NA_i^2$

$$V = 2\pi^2 \sum_{i=1}^{N} \frac{\rho_i^2 - \rho_{i-1}^2}{2} NA_i^2 \tag{3}$$

where n_i is the refractive index and ρ_i is the outer radius of the ith layer ($\rho_0 = 0$).

When joining two fibers, we can characterize the transmitting and receiving fibers by different profiles ($\rho_{1,t}, \rho_{2,t}, \ldots, \rho_{N,t}$,

$NA_{1,t}, NA_{2,t}, \ldots, NA_{N,t})$ and $(\rho_{1,r}, \rho_{2,r}, \ldots, \rho_{N,r}, NA_{1,r}, NA_{2,r}, \ldots, NA_{N,r})$, respectively. Using the notation above, the total mode volumes of the transmitting and receiving fibers can be expressed as

$$V_t = 2\pi^2 \sum_{i=1}^{N} \frac{\rho_{i,t}^2 - \rho_{i-1,t}^2}{2} NA_{i,t}^2 \tag{4}$$

and

$$V_r = 2\pi^2 \sum_{i=1}^{N} \frac{\rho_{i,r}^2 - \rho_{i-1,r}^2}{2} NA_{i,r}^2. \tag{5}$$

The magnitude of the insertion loss when considering tolerances to each core surface diameter and each numerical aperture can be analytically evaluated if the following assumptions are made.

1) Power is uniformly distributed over all modes.
2) The transmitting and receiving fibers have the same number of layers N.
3) The radii of each layer for both transmitting and receiving fibers satisfy

$$\begin{cases} 0 \leqslant \rho_{1,r} \leqslant \rho_{2,t}, & i = 1 \\ \rho_{i-1,t} \leqslant \rho_{i,r} \leqslant \rho_{i+1,t}, & i = 2, \ldots, N-1 \\ \rho_{N-1,t} \leqslant \rho_{N,r}, & i = N \end{cases}.$$

With these requirements, the common mode volume V_{rt}, expressed as the fraction of the mode volume of the transmitting fiber transferred to the receiving fiber, can be calculated as (see the Appendix for further explanation)

$$\begin{aligned} V_{rt} = 2\pi^2 \sum_{i=1}^{N} \Bigg(& \min\left\{NA_{i-1,p}^2, NA_{i,q}^2\right\} \\ & \times \frac{\max\left\{\rho_{i-1,r}^2, \rho_{i-1,t}^2\right\} - \min\left\{\rho_{i-1,r}^2, \rho_{i-1,t}^2\right\}}{2} \\ & + \min\left\{NA_{i,r}^2, NA_{i,t}^2\right\} \\ & \times \frac{\min\left\{\rho_{i,r}^2, \rho_{i,t}^2\right\} - \max\left\{\rho_{i-1,r}^2, \rho_{i-1,t}^2\right\}}{2} \Bigg) \end{aligned} \tag{6}$$

where $\rho_{0,r} = 0$, $\rho_{0,t} = 0$, $NA_{0,r} = 0$, $NA_{0,t} = 0$, and the following cases must be considered, i.e.,

$$\text{if } \rho_{i-1,t} \geqslant \rho_{i-1,r} \begin{cases} p = t \\ q = r \end{cases}$$

$$\text{which would lead to } \begin{cases} NA_{i-1,p}^2 = NA_{i-1,t}^2 \\ NA_{i,q}^2 = NA_{i,r}^2 \end{cases}$$

$$\text{if } \rho_{i-1,t} < \rho_{i-1,r} \begin{cases} p = r \\ q = t \end{cases}$$

$$\text{which would lead to } \begin{cases} NA_{i-1,p}^2 = NA_{i-1,r}^2 \\ NA_{i,q}^2 = NA_{i,t}^2 \end{cases}.$$

Finally, by substituting V_{rt} for (6) and V_t for (4), the coupling loss L_{MSI} is calculated as

$$L_{\mathrm{MSI}} = -10 \log \frac{V_{rt}}{V_t}. \tag{7}$$

Constraint 3) in the assumptions above can be relaxed, even though it would not be possible any longer to obtain a compact analytical expression to calculate the intrinsic coupling loss for an MSI fiber. Instead, a computer model should be implemented. The flow chart in Fig. 1 shows a very simple algorithm to compute V_{rt} with

$$A = \min\left\{NA_{q,r}^2, NA_{p,t}^2\right\} \frac{\min\left\{\rho_{q,r}^2, \rho_{p,t}^2\right\}}{2} \tag{8}$$

$$B = \min\left\{NA_{q,r}^2, NA_{p,t}^2\right\} \frac{\min\left\{\rho_{q,r}^2, \rho_{p,t}^2\right\} - \rho_{q-1,r}^2}{2} \tag{9}$$

$$C = \min\left\{NA_{q,r}^2, NA_{p,t}^2\right\} \frac{\min\left\{\rho_{q,r}^2, \rho_{p,t}^2\right\} - \rho_{p-1,t}^2}{2} \tag{10}$$

and

$$\begin{aligned} D = & \min\left\{NA_{q,r}^2, NA_{p,t}^2\right\} \\ & \times \frac{\min\left\{\rho_{q,r}^2, \rho_{p,t}^2\right\} - \max\left\{\rho_{q-1,r}^2, \rho_{p-1,t}^2\right\}}{2}. \end{aligned} \tag{11}$$

Finally, it is straightforward to show that, for $N = 1$, (7) reduces to the intrinsic coupling loss for an SI fiber, which can be further split into two separate expressions related to the coupling loss attributable to mismatches in core diameters and in numerical apertures, respectively, as stated in [8]

$$L_\rho = \begin{cases} -10 \log \left(\frac{\rho_{1,r}}{\rho_{1,t}}\right)^2, & \text{if } \rho_{1,r} < \rho_{1,t} \\ 0, & \text{if } \rho_{1,r} \geqslant \rho_{1,t} \end{cases} \tag{12}$$

$$L_{NA} = \begin{cases} -10 \log \left(\frac{NA_{1,r}}{NA_{1,t}}\right)^2, & \text{if } NA_{1,r} < NA_{1,t} \\ 0, & \text{if } NA_{1,r} \geqslant NA_{1,t} \end{cases}. \tag{13}$$

III. Validation of the Results Obtained by Using Analytical Expressions

In order to establish the validity of the expressions obtained before, several computer simulations have been carried out to obtain the intrinsic coupling losses for SI, GI, and MSI fibers, and have been compared with the results obtained by using the ray-tracing method under the same conditions [6]. These computer simulations consist in evaluating the intrinsic coupling losses due to tolerances in core diameter ρ_N, peak numerical aperture $NA(0) = NA_1$, and refractive index profile exponent g (only for GI fibers), which were assumed to follow a normal distribution [7].

A. Structural Characteristics of the Analyzed Fibers

In the statistical analyses carried out for SI and clad parabolic profile GI fibers, we have chosen the value of 1.492 as the

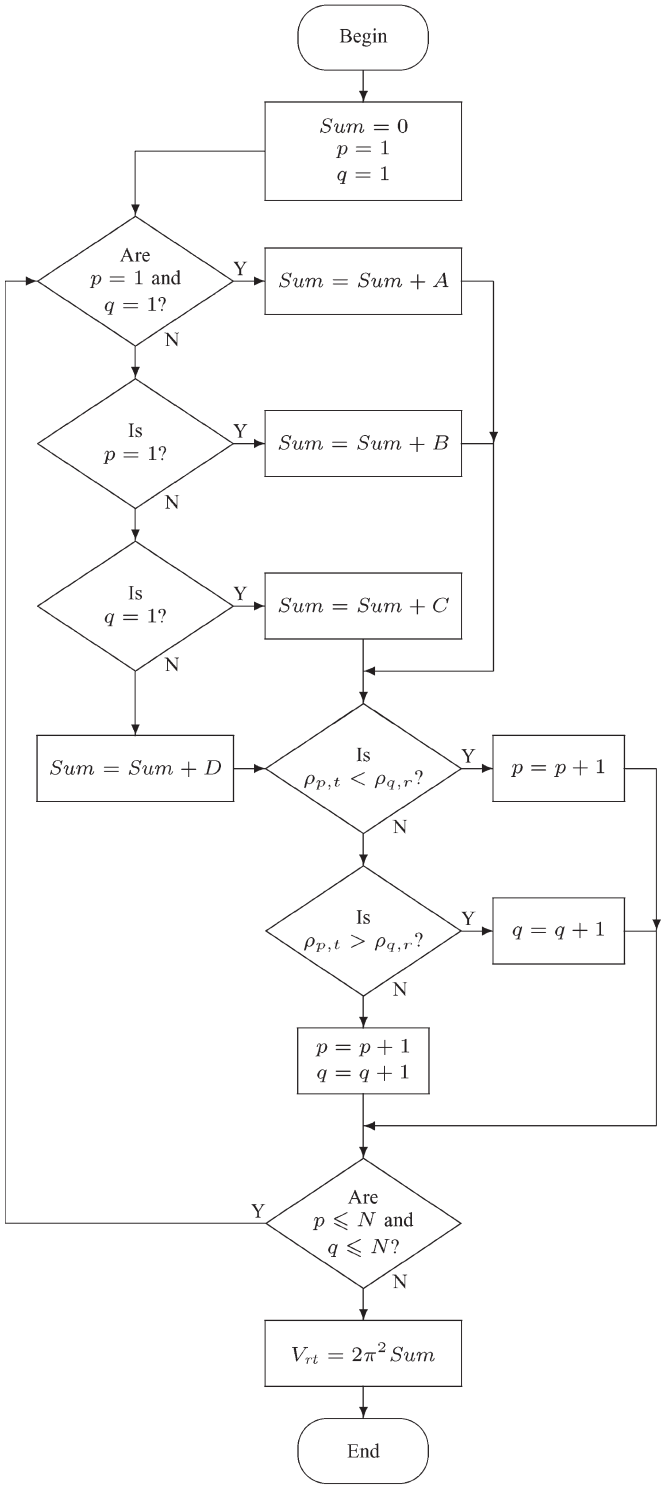

Fig. 1. Flow chart showing the algorithm that allows computation of V_{rt} without any restriction on the radii of each layer for both transmitting and receiving MSI fibers. A, B, C, and D are given by (8)–(11), respectively.

highest refractive index in the core $(n(0) = n_{co})$ and 1.402 as the refractive index of the cladding (n_{cl}), yielding a peak numerical aperture $(NA(0))$ of 0.51 for the transmitting fiber. The radius of the core of the transmitting fiber has been set to $\rho = 490$ μm.

It is worthy of remark that, as stated in [6], the values above can be arbitrarily chosen. This is possible because each of the fiber parameter variations is normalized to its respective parameter and, therefore, the results obtained are the same, even if the fiber dimensions or the material properties are scaled to greater or lower values (in the framework of the classical geometric optics). In consequence, the results obtained can be considered to be valid for any kind of highly multimode optical fiber used as a transmission medium.

For the sake of comparison, it is also interesting to note that an MSI fiber can be used as an approach of any kind of GI fiber, provided that it has a sufficiently high number of layers N, by maintaining the width of each layer constant (i.e., $\rho_i - \rho_{i-1} =$ constant $\forall i$) and fitting the refractive indices of the MSI fiber in such a way that the overall refractive index profile approximates to that of the GI fiber, i.e.,

$$n_{\mathrm{MSI},i} = n_{\mathrm{GI}}(r)\Big|_{r=\rho_{i-1}} \qquad \forall i.$$

For instance, Fig. 2(a) shows the resultant parabolic refractive index profile for an MSI fiber of $N = 10$ layers, superimposed on the profile corresponding to a parabolic profile GI fiber (whose refractive index profile exponent g has been adjusted to $g = 2$).

Furthermore, we have taken two different MSI-POFs in order to compare the statistical results calculated analytically with those obtained by using the ray-tracing method in real MSI fibers, namely the Eska–Miu fiber from Mitsubishi [10] and the MSI-POF from TVER [11]. The former has three layers, the innermost one being fairly thick and the outermost one extremely thin, whereas the latter has four layers, three of them of similar thickness. The physical dimensions of the different layers are reproduced in Table I. Fig. 2(b) and (c) shows, in addition, their respective refractive index profiles measured with the aid of the inverse near-field method [12], [13].

For the MSI fibers investigated in this paper, we have taken the value of 1.492 as the refractive index of the innermost layer (n_1), considering a value of 1.402 as the refractive index of the cladding (n_{cl}). The refractive indices of the remaining layers in between are adjusted according to the measured refractive index profiles in Fig. 2 relative to the extreme values n_1 and n_{cl}. On the other hand, the radius corresponding to the outermost layer of the parabolic profile MSI fiber has been chosen to be 490 μm.

B. Set-Up of the Computer Simulations

We have run a set of computer simulations of 50 000 trials that involves joining two fibers randomly chosen from a given population following a normal distribution. We have evaluated the resultant intrinsic coupling loss when only one of the possible structural parameters is varied (namely, the numerical aperture or the core diameter, or the refractive index profile exponent g in case of GI fibers) and also when the mismatches are applied all together. Each parameter has a normalized standard deviation of 5%.

As mentioned in [6], it should be noted that the probability of obtaining too extreme parameters as a result of making use of normally distributed random deviations is virtually negligible.

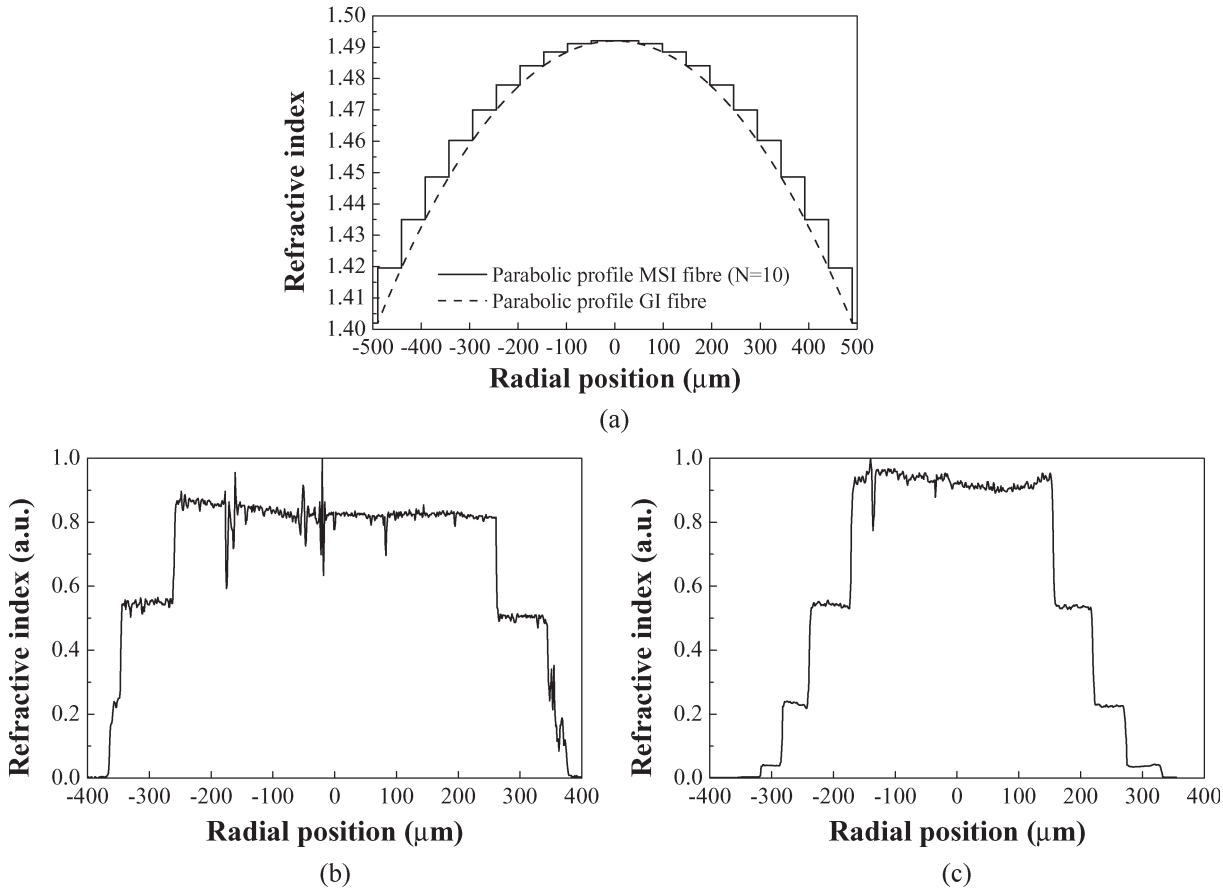

Fig. 2. Refractive index profiles corresponding to the MSI fibers used. (a) Parabolic profile MSI fiber $(N = 10)$. (b) Eska–Miu fiber. (c) TVER fiber.

TABLE I
PHYSICAL DIMENSIONS OF THE DIFFERENT LAYERS (OUTER RADII IN MILLIMETER)

	Layer 1	Layer 2	Layer 3	Layer 4
Eska-Miu	0.25	0.35	0.38	–
TVER	0.16	0.23	0.27	0.33

Consider, for instance, the probability of coming across a random deviation outside an interval defined by four standard deviations. This value turns out to be of only 0.006%, so we can only expect to find approximately fewer than three samples exceeding the value of this mismatch after each set of computer simulations of 50 000 trials, i.e., their effect can be considered practically negligible. Notice that for the normalized standard deviations chosen for each parameter the corresponding percentile value of the mismatch is $4 \times 0.05 = 0.2 = 20\%$, which, though certainly high, is still perfectly plausible. This fact can be ascertained by calculating and assessing the percentile value corresponding to the limit points of the interval of the probability function out of which, statistically, only one sample out of 50 000 trials is expected. Indeed, this turns out to be equal to 4.265 standard deviations, that is, 21.325%, a value completely plausible.

Taking into account that MSI fibers consist of several layers and, therefore, the number of parameters that are liable to vary grows as the number of layers increases, we have adopted two different approaches to the statistical evaluation of intrinsic coupling losses for this kind of fibers:

1) applying the same normalized deviation to each waveguide parameter on every layer;
2) applying a different normalized deviation to each waveguide parameter on each layer.

In the former case, once the normalized deviation of a certain parameter (either the numerical aperture of the innermost layer or the radius of the outermost layer) has been randomly chosen from a normal distribution on each trial, the parameters corresponding to the rest of the layers are calculated according to the same normalized deviation. This is the most appropriate situation when attempting to compare parabolic profile MSI fibers with clad parabolic profile GI fibers.

In the latter case, the procedure for the random building of the receiving fiber on each trial is summarized elsewhere [6], in which the only waveguide parameters randomly chosen from a normal distribution are the numerical aperture and the outer radius of each layer. In Section III-C, we will study the effects on intrinsic coupling loss of more realistic constraints imposed on the building of the receiving fiber and their influence as the number of layers increases. We believe that this situation describes the effects of mismatches that in fact may occur during manufacturing processes better than the previous approach.

As for the statistical computations concerned in the method of solving the intrinsic coupling losses, whereas the analytical expressions used for SI fibers are given by (12) and (13), for

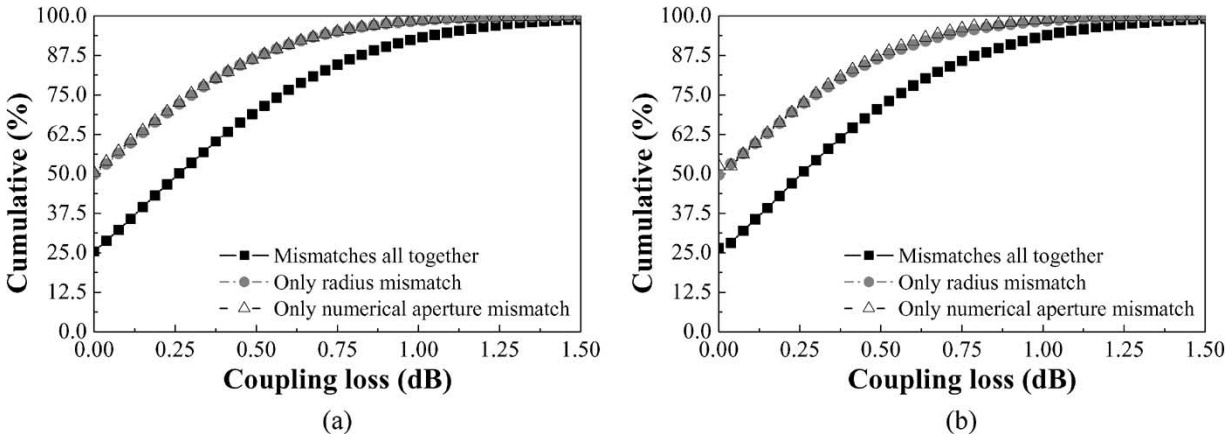

Fig. 3. SI fiber. Cumulative percentage of fiber joints having intrinsic coupling losses below a given value. (a) Analytical results. (b) Ray-tracing results.

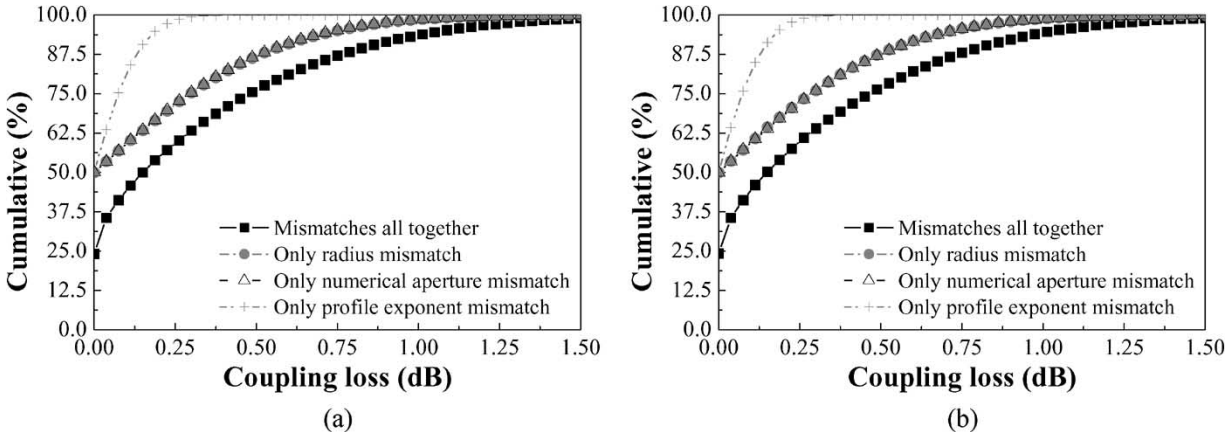

Fig. 4. Clad parabolic profile GI fiber. Cumulative percentage of fiber joints having intrinsic coupling losses below a given value. (a) Analytical results. (b) Ray-tracing results.

MSI fibers we have used (7) with V_{rt} calculated using either (6) or the computer algorithm shown in Fig. 1. The way to calculate V_{rt} depends on whether the normalized deviation of each waveguide parameter is the same on every layer or not. With regard to GI fibers, in the Appendix, we provide a more detailed explanation of how to calculate the intrinsic coupling loss from the common mode volume analytically.

On the other hand, when using the ray-tracing method, we have launched approximately 200 000 rays from a hypothetical source covering the whole input surface of the transmitting fiber and emitting a uniform mode distribution (UMD) with a numerical aperture $NA_{\text{input}} = 0.57$ (thus ensuring that the launched rays will fill the effective solid acceptance angle of the transmitting fiber). This number of rays, although lower than the upper boundary delimited by the total number of modes that can propagate within the fibers, is high enough to ensure sufficiently smooth and accurate results. The former is calculated from the waveguide parameter V [14].

Finally, it is important to bear in mind that any conclusion derived from this analysis should, nevertheless, be interpreted carefully, since the results in Section III-C are obtained assuming a uniform distribution of energy over all modes. Even though such an assumption limits the extended application of the analytical expressions to more realistic conditions (which have a strong influence on coupling losses [15]), the results obtained by evaluating the analytical expressions are still useful for assessing fiber quality. This is so because a uniform power distribution constitutes the worst case and leads, in some way, to quite conservative estimates of the coupling efficiency. Therefore, it is expected that coupling losses obtained under more realistic conditions, such as in the case of having restricted launching conditions or when including the modifications induced in the light power distribution by mode mixing, will never be higher than the limit values given by the analytical expressions, so we can conclude that the analytical calculations provide an upper bound for coupling losses.

C. Results and Discussion

First of all, we have checked whether the results obtained from the analytical expressions and from the ray-tracing method are comparable or not. This task has been carried out by running several computer simulations for SI and clad parabolic profile GI fibers and computing the resultant intrinsic coupling losses. The results are shown in Figs. 3 and 4, where the ordinate shows the cumulative percentage of fiber joints that have intrinsic coupling losses lower than the value given in the abscissa.

The details of the 50% loss L_{50}, or median loss, and the 90% loss L_{90} are shown in Tables II and III. The 50% loss L_{50}

TABLE II
SI FIBER. STATISTICAL RESULTS OBTAINED FOR 50% LOSS L_{50} AND 90% LOSS L_{90} BY USING ANALYTICAL EXPRESSIONS AND RAY-TRACING METHOD

	Analytical results		**Ray-tracing results**	
	L_{50}(dB)	L_{90}(dB)	L_{50}(dB)	L_{90}(dB)
Mismatches all together	0.26	0.89	0.249	0.867
Only radius mismatch	0.001	0.574	0.004	0.575
Only numerical aperture mismatch	0.0	0.575	0.0	0.541

TABLE III
CLAD PARABOLIC PROFILE GI FIBER. STATISTICAL RESULTS OBTAINED FOR 50% LOSS L_{50} AND 90% LOSS L_{90} BY USING ANALYTICAL EXPRESSIONS AND RAY-TRACING METHOD

	Analytical results		**Ray-tracing results**	
	L_{50}(dB)	L_{90}(dB)	L_{50}(dB)	L_{90}(dB)
Mismatches all together	0.149	0.842	0.148	0.812
Only radius mismatch	0.0	0.577	0.0	0.55
Only numerical aperture mismatch	0.0	0.571	0.0	0.556
Only profile exponent mismatch	0.0	0.145	0.0	0.14

denotes that 50% of the samples considered in a large statistical population of fibers following a normal distribution will have a value of intrinsic coupling loss below L_{50}. The same applies to the 90% loss L_{90}.

It can be observed that the obtained results are in excellent agreement and, since the theoretical expressions corresponding to this kind of fibers have been previously checked [8], we can safely compare the results obtained using both methods in order to validate our analytical expressions for MSI fibers later. Please notice that the slight variations in the results shown in Tables II and III are solely due to the statistical nature of the set of measurements carried out in the computer simulations.

Another three conclusions can also be drawn from the results displayed above (Figs. 3 and 4), which are analyzed in more detail in [6]. First, coupling loss when considering the mismatches all together is neither the sum of the coupling losses due to each parameter variation nor the quadratic mean of them. Second, coupling loss when considering the mismatches all together is slightly higher for SI fibers than for GI ones. Third, for clad parabolic profile GI fibers, mismatches in their refractive index profile exponents lead to much lower coupling losses.

Figs. 5 and 6 show the results obtained for the intrinsic coupling loss when only one of the parameters is varied and also when the mismatches are applied all together, both for the Eska–Miu MSI-POF and for the parabolic profile MSI fiber of $N = 10$ layers (in view of the similar conclusions drawn from the plots corresponding to the Eska–Miu and TVER MSI-POFs, the graphical results obtained for the latter are not shown here).

The details of the 50% loss L_{50}, or median loss, and the 90% loss L_{90} for each type of fiber (including the TVER fiber) are shown in Tables IV–VI.

Again, it can be observed that the results obtained using the analytical expressions coincide almost exactly with those obtained using the ray-tracing method save the obvious minimal statistical fluctuations. Furthermore, this coincidence happens for every MSI fiber regardless of the approach used for the statistical evaluation of intrinsic coupling losses, i.e., the results match up irrespective of whether we use or not the same normalized deviation for each waveguide parameter on every layer.

However, there are two details that do not go unnoticed. First of all, it is evident from Tables IV–VI that the 90% loss L_{90} obtained when using different normalized deviations on each layer is certainly lower than the 90% loss obtained for the same normalized deviations on every layer, whereas the behavior of the 50% loss L_{50} is just the opposite. This effect is especially noticeable if we consider the mismatches all together. In order to understand the reason for having such a behavior, we have to analyze how the random deviations following a normal distribution are applied to each waveguide parameter in each of the approaches considered. In both cases, we have the same probabilities of coming across a positive or negative random deviation. A negative one (meaning that the receiving fiber has a lower numerical aperture or a smaller core diameter) produces some loss, whereas a positive one leads to no loss at all. However, if we consider the approach in which the same normalized deviation is applied to each waveguide parameter on every layer, then a negative normalized deviation will negatively affect the rest of the layers. In contrast, if we now consider the approach in which a different normalized deviation is applied to each waveguide parameter on each layer, then the fact that a negative deviation has occurred on a certain layer does not imply that the same will happen on the rest of the layers. For this reason, it is expected that the 90% loss L_{90} obtained for the latter approach will be more optimistic than that for the former one. A similar reasoning applies to the median loss L_{50}, since a positive random deviation (its probability being the same as that of a negative one) obtained for a certain waveguide parameter will have a more positive effect (for the population of fiber joints having losses below L_{50}) when the deviation is applied to every layer of the fiber, and a more negative effect when entirely different random deviations are applied.

Second, the other fact that attracts our attention lies in the results obtained for the parabolic profile MSI fiber of $N = 10$ layers when using different normalized deviations on each layer, as shown in Fig. 6(c) [or Fig. 6(d)] and Table VI. Indeed, an unusually low coupling loss is obtained when considering only numerical aperture mismatches, in comparison with the results for core diameter mismatches only. As a matter of fact, previous results and (7), with V_{rt} calculated using the computer algorithm shown in Fig. 1, suggest that coupling losses should have been of the same order of magnitude [we could come to the same conclusion even if we only analyzed (6)]. The explanation for such disagreement can be found in the stricter limitations imposed on the building of the refractive index profile of the receiving fiber. As it is evident from Fig. 2(a), the accepted margins allowed for the normally distributed random deviations in the refractive indices are much

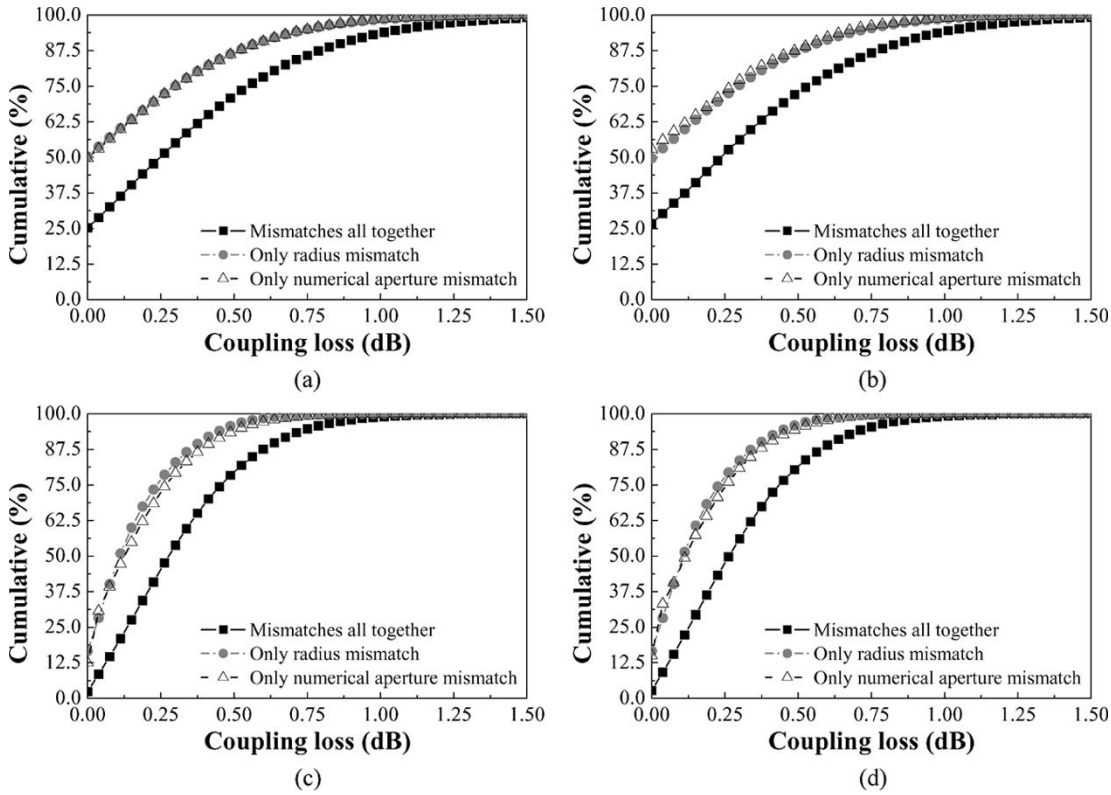

Fig. 5. Eska–Miu fiber. Cumulative percentage of fiber joints having intrinsic coupling losses below a given value. (a) Analytical results obtained using the same normalized deviations on every layer. (b) Ray-tracing results obtained using the same normalized deviations on every layer. (c) Analytical results obtained using different normalized deviations on each layer. (d) Ray-tracing results obtained using different normalized deviations on each layer.

narrower on the innermost layers than on the outermost ones, whereas these margins are the same for any outer radius, irrespective of the layer. It is of fundamental importance to bear in mind that if such margins are exceeded the trial is aborted and the value outside the scope is replaced with a new random choice, that is, there is a truncation of the normal distribution. For instance, in one of the 50 000 trials, the normalized mean value of the numerical apertures randomly generated for the innermost layer of the receiving fiber shifted from zero to a positive value of 0.08, whereas the corresponding normalized standard deviation was 0.04 instead of the set value of 0.05. As a consequence, we expect a more conservative estimate of the coupling efficiency when considering only numerical aperture mismatches than for core diameter mismatches alone. Obviously, this will also have an effect on the results obtained when mismatches are applied all together.

Instead, it is particularly interesting to note that the results obtained for a parabolic profile MSI fiber of $N = 10$ layers when using the same normalized deviations on every layer are almost the same as those obtained for a clad parabolic profile GI fiber, as can be observed from direct comparison of the sets of Figs. 4(a) and 6(a) [or Figs. 4(b) and 6(b)], as well as in Tables III and VI.

There is also another interesting feature that can be inferred from the statistical results obtained for the three different MSI fibers investigated when using different normalized deviations on each layer. Specifically, the 90% loss L_{90} of Tables IV and V obtained using different normalized deviations on each layer (either from the analytical results or from the ray-tracing ones) shows that coupling loss for the TVER fiber is slightly lower than that for the Eska–Miu fiber (which has one less layer). Coupling loss for the parabolic profile MSI fiber of $N = 10$ layers is even much lower than for the Eska–Miu or the TVER fibers, as can be seen in Table VI, even though it should be emphasized that this marked decrease is due, in part, to the truncations whose effects have already been discussed above. All in all, this result suggests that, as the number of layers of an MSI fiber increases, there is a slight improvement in the coupling loss for a given percentage of fiber joints, even though this is practically indistinguishable. For the median loss L_{50}, the very weak dependence of coupling losses on the number of layers becomes masked by the inherent statistical fluctuations since the value of L_{50} is not sufficiently high in magnitude to overcome such effects.

D. Comparison With Other Results Available in the Literature

Finally, we have attempted to compare our simulation results with the measurements performed by Thiel and Davis [7] and to assess how well an MSI fiber can be approximated to a GI fiber in terms of intrinsic coupling losses.

Fig. 7 shows the results obtained with 50 000 trials for SI fibers, clad power-law profile GI fibers, and MSI fibers of $N = 10$ and $N = 100$ layers, whose overall refractive index profiles have been fitted using the same refractive index profile exponents g of the clad power-law profile GI fibers. The values chosen for the core radius (the outermost layer in the case of MSI fibers), the peak numerical aperture, and the refractive

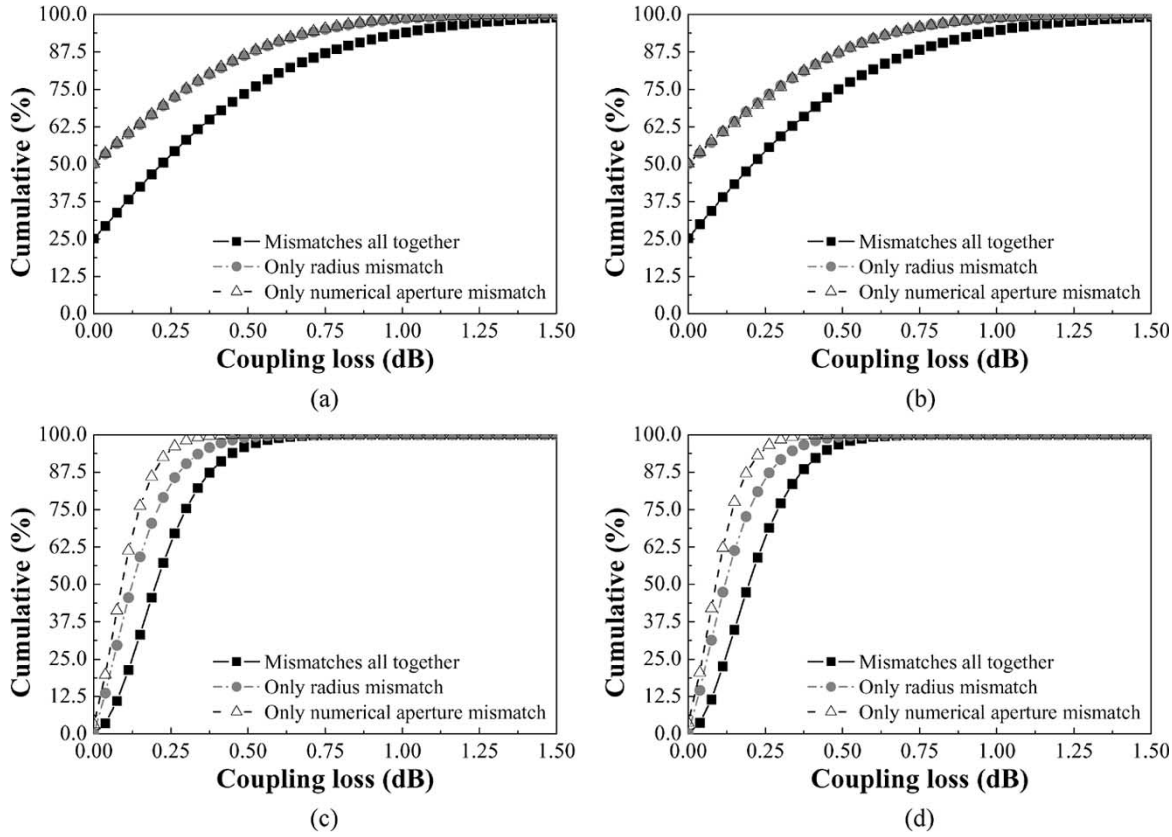

Fig. 6. Parabolic profile MSI fiber ($N = 10$). Cumulative percentage of fiber joints having intrinsic coupling losses below a given value. (a) Analytical results obtained using the same normalized deviations on every layer. (b) Ray-tracing results obtained using the same normalized deviations on every layer. (c) Analytical results obtained using different normalized deviations on each layer. (d) Ray-tracing results obtained using different normalized deviations on each layer.

TABLE IV
ESKA–MIU FIBER. STATISTICAL RESULTS OBTAINED FOR 50% LOSS L_{50} AND 90% LOSS L_{90} BY USING ANALYTICAL EXPRESSIONS AND RAY-TRACING METHOD

Results obtained using the same normalized deviations on every layer				
	Analytical results		**Ray-tracing results**	
	L_{50}(dB)	L_{90}(dB)	L_{50}(dB)	L_{90}(dB)
Mismatches all together	0.248	0.862	0.235	0.837
Only radius mismatch	0.0	0.575	0.003	0.562
Only numerical aperture mismatch	0.003	0.579	0.0	0.536

Results obtained using different normalized deviations on each layer				
	Analytical results		**Ray-tracing results**	
	L_{50}(dB)	L_{90}(dB)	L_{50}(dB)	L_{90}(dB)
Mismatches all together	0.276	0.64	0.263	0.617
Only radius mismatch	0.109	0.382	0.107	0.373
Only numerical aperture mismatch	0.125	0.423	0.114	0.401

TABLE V
TVER FIBER. STATISTICAL RESULTS OBTAINED FOR 50% LOSS L_{50} AND 90% LOSS L_{90} BY USING ANALYTICAL EXPRESSIONS AND RAY-TRACING METHOD

Results obtained using the same normalized deviations on every layer				
	Analytical results		**Ray-tracing results**	
	L_{50}(dB)	L_{90}(dB)	L_{50}(dB)	L_{90}(dB)
Mismatches all together	0.244	0.871	0.243	0.849
Only radius mismatch	0.0	0.577	0.001	0.559
Only numerical aperture mismatch	0.0	0.576	0.0	0.559

Results obtained using different normalized deviations on each layer				
	Analytical results		**Ray-tracing results**	
	L_{50}(dB)	L_{90}(dB)	L_{50}(dB)	L_{90}(dB)
Mismatches all together	0.302	0.624	0.295	0.608
Only radius mismatch	0.146	0.357	0.141	0.347
Only numerical aperture mismatch	0.13	0.406	0.127	0.398

index profile exponent (only for clad power-law profile GI fibers and MSI fibers with the same g profile), as well as their normalized standard deviations, are shown in the inset. It should be kept in mind that, for the MSI fibers considered, once the normalized deviation of a certain parameter has been randomly chosen from a normal distribution on each trial (such as the numerical aperture of the innermost layer or the radius of the outermost layer), the parameters corresponding

TABLE VI
PARABOLIC PROFILE MSI FIBER ($N = 10$). STATISTICAL RESULTS OBTAINED FOR 50% LOSS L_{50} AND 90% LOSS L_{90} BY USING ANALYTICAL EXPRESSIONS AND RAY-TRACING METHOD

Results obtained using the same normalized deviations on every layer

	Analytical results		**Ray-tracing results**	
	L_{50}(dB)	L_{90}(dB)	L_{50}(dB)	L_{90}(dB)
Mismatches all together	0.219	0.838	0.209	0.807
Only radius mismatch	0.0	0.574	0.0	0.548
Only numerical aperture mismatch	0.0	0.572	0.0	0.553

Results obtained using different normalized deviations on each layer

	Analytical results		**Ray-tracing results**	
	L_{50}(dB)	L_{90}(dB)	L_{50}(dB)	L_{90}(dB)
Mismatches all together	0.201	0.4	0.195	0.389
Only radius mismatch	0.124	0.296	0.119	0.284
Only numerical aperture mismatch	0.09	0.208	0.089	0.203

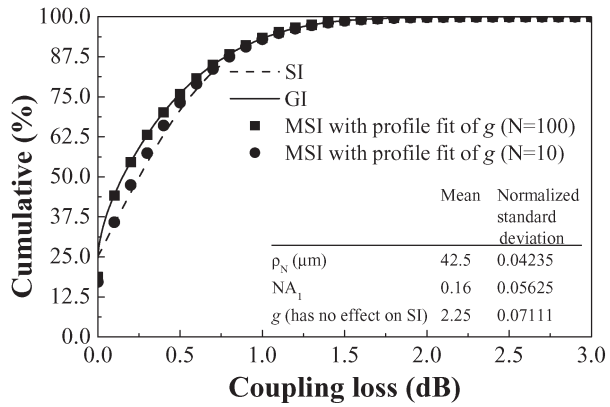

Fig. 7. Cumulative percentage of fiber joints having intrinsic coupling losses below a given value. Results obtained for simulations of 50 000 trials by using the analytical expressions of the common mode volume. SI fibers and clad power-law profile GI and MSI fibers.

to the rest of the layers are calculated according to the same normalized deviation. Please also notice that, considering again the probability of coming across a random deviation outside an interval defined by four standard deviations (which is of only 0.006%, i.e., virtually negligible), for the chosen normalized standard deviations of the core radius, of the peak numerical aperture, and of the refractive index profile exponent in Fig. 7, the corresponding percentile values are 17%, 22%, and 28.44%, respectively, and, therefore, completely plausible.

The details of the 50% loss L_{50}, or median loss, and the 90% loss L_{90} for each type of fiber are shown in Table VII.

For some reason, there are discrepancies between our results for clad power-law GI fibers and those obtained by Thiel and Davis [7] (0.151 dB against 0.2 dB for the median loss L_{50} and 0.858 dB against 1.15 dB for the 90% loss L_{90}), even though we have made sure that we have reproduced exactly the same calculations under the same conditions. In any case, the results

TABLE VII
STATISTICAL RESULTS OBTAINED FOR 50% LOSS L_{50} AND 90% LOSS L_{90} BY USING ANALYTICAL EXPRESSIONS OF THE COMMON MODE VOLUME

	L_{50}(dB)	L_{90}(dB)
SI fibre	0.252	0.89
Clad power-law profile GI fibre	0.151	0.858
MSI fibre with profile fit of exponent g ($N = 100$)	0.153	0.857
MSI fibre with profile fit of exponent g ($N = 10$)	0.223	0.878

previously discussed in Section III-C and the excellent agreement between our statistical results for the clad power-law GI fiber and for the MSI fiber of $N = 100$ layers serve to ascertain that our analytical expressions for the common mode volume have been correctly solved. This is clear in view of the different approaches that were taken to work out the answers, as can be observed in Section II and in the Appendix. Therefore, we attribute these discrepancies to the better computer simulation techniques that are available nowadays.

On the other hand, it is clear from Fig. 7 that the results obtained for the MSI fibers are consistent with the fact that the number of layers of an MSI fiber has some slight influence on coupling loss.

IV. CONCLUSION

We have obtained the theoretical expressions that allow a straightforward calculation of intrinsic coupling loss for MSI fibers under the assumption of a uniform power distribution across the light cone of radiation defined by the input numerical aperture, which constitutes the worst-case scenario. These expressions do not only lack the complicated mathematical procedures that would be a major obstacle to their implementation on any programmable pocket calculator but also provide an upper bound for coupling losses. As a consequence, this property ensures that measurements obtained under more realistic conditions will always be well below these limit values. We have validated our theoretical model by carrying out several statistical analyses involving computer simulations in order to evaluate intrinsic coupling loss when joining two fiber ends and by comparing them with the results obtained using the ray-tracing method or with those available in the literature. The obtained results have also served us to find out that there is an inverse relationship, though very slight, between the number of layers of an MSI fiber and the value of the coupling loss.

APPENDIX
ANALYTICAL EXPRESSIONS OF THE COMMON MODE VOLUME FOR GI FIBERS AND COMPARISON WITH MSI FIBERS

GI fibers with clad power-law profiles are defined by [16]

$$n^2(r) = \begin{cases} n_{co}^2\left[1 - 2\Delta\left(\frac{r}{\rho}\right)^g\right], & r \leqslant \rho \\ n_{co}^2[1 - 2\Delta] = n_{cl}^2, & r > \rho \end{cases} \tag{A1}$$

TABLE VIII
ANALYTICAL EXPRESSIONS OF THE COMMON MODE VOLUME $V_{\mathrm{GI}_{rt}}$ FOR CLAD POWER-LAW PROFILE GI FIBERS

Without intersections
$\min\{V_{GI_t}, V_{GI_r}\} = \min\left\{2\pi^2 NA_t^2(0)\,\rho_t^2 \dfrac{g_t}{2(2+g_t)}, 2\pi^2 NA_r^2(0)\,\rho_r^2 \dfrac{g_r}{2(2+g_r)}\right\}$
Only one intersection
$\begin{cases} 2\pi^2 NA_r^2(0)\,\rho_r^2 \int_0^{r_{IP1}/\rho_r} [1-r^{g_r}]\,r\mathrm{d}r + 2\pi^2 NA_t^2(0)\,\rho_t^2 \int_{r_{IP1}/\rho_t}^{1} [1-r^{g_t}]\,r\mathrm{d}r & \text{if } \left(NA_t^2(0)\,[1-(r/\rho_t)^{g_t}]\,r - NA_r^2(0)\,[1-(r/\rho_r)^{g_r}]\,r\right)\Big\|_{r<r_{IP1}} > 0 \\ 2\pi^2 NA_t^2(0)\,\rho_t^2 \int_0^{r_{IP1}/\rho_t} [1-r^{g_t}]\,r\mathrm{d}r + 2\pi^2 NA_r^2(0)\,\rho_r^2 \int_{r_{IP1}/\rho_r}^{1} [1-r^{g_r}]\,r\mathrm{d}r & \text{if } \left(NA_t^2(0)\,[1-(r/\rho_t)^{g_t}]\,r - NA_r^2(0)\,[1-(r/\rho_r)^{g_r}]\,r\right)\Big\|_{r<r_{IP1}} < 0 \end{cases}$
Two intersections
$\begin{cases} 2\pi^2 NA_r^2(0)\,\rho_r^2 \int_0^{r_{IP1}/\rho_r} [1-r^{g_r}]\,r\mathrm{d}r + 2\pi^2 NA_t^2(0)\,\rho_t^2 \int_{r_{IP1}/\rho_t}^{r_{IP2}/\rho_t} [1-r^{g_t}]\,r\mathrm{d}r + 2\pi^2 NA_r^2(0)\,\rho_r^2 \int_{r_{IP2}/\rho_r}^{1} [1-r^{g_r}]\,r\mathrm{d}r & \text{if } \left(NA_t^2(0)\,[1-(r/\rho_t)^{g_t}]\,r - NA_r^2(0)\,[1-(r/\rho_r)^{g_r}]\,r\right)\Big\|_{r<r_{IP1}} > 0 \\ 2\pi^2 NA_t^2(0)\,\rho_t^2 \int_0^{r_{IP1}/\rho_t} [1-r^{g_t}]\,r\mathrm{d}r + 2\pi^2 NA_r^2(0)\,\rho_r^2 \int_{r_{IP1}/\rho_r}^{r_{IP2}/\rho_r} [1-r^{g_r}]\,r\mathrm{d}r + 2\pi^2 NA_t^2(0)\,\rho_t^2 \int_{r_{IP2}/\rho_t}^{1} [1-r^{g_t}]\,r\mathrm{d}r & \text{if } \left(NA_t^2(0)\,[1-(r/\rho_t)^{g_t}]\,r - NA_r^2(0)\,[1-(r/\rho_r)^{g_r}]\,r\right)\Big\|_{r<r_{IP1}} < 0 \end{cases}$

where the value of Δ is the relative difference between indices

$$\Delta = \frac{n_{co}^2 - n_{cl}^2}{2n_{co}^2} \tag{A2}$$

and the factor g is the so-called refractive index profile exponent of the optical fiber.

The local numerical aperture $NA(r)$ for these fibers can be rewritten as

$$NA^2(r) = NA^2(0)\left[1 - \left(\frac{r}{\rho}\right)^g\right] \tag{A3}$$

where $NA(0)$ is the peak numerical aperture defined as

$$NA(0) = \left(n_{co}^2 - n_{cl}^2\right)^{\frac{1}{2}}.$$

As stated in [7], the mode volume of a clad power-law profile GI fiber between radii r_A and $r_B > r_A$ can be expressed as

$$\begin{aligned} V_{\mathrm{GI}} &= 2\pi^2 NA^2(0) \int_{r_A}^{r_B} \left[1 - \left(\frac{r}{\rho}\right)^g\right] r\,dr \\ &= 2\pi^2 NA^2(0)\rho^2 \int_{\frac{r_A}{\rho}}^{\frac{r_B}{\rho}} [1 - r^g]\,r\,dr. \end{aligned} \tag{A4}$$

The total mode volume $V_{\mathrm{GI}_{\mathrm{total}}}$ of a clad power-law profile GI fiber can be analytically solved, yielding

$$V_{\mathrm{GI}_{\mathrm{total}}} = 2\pi^2 NA^2(0)\rho^2 \frac{g}{2(2+g)}. \tag{A5}$$

Nonetheless, there is no closed-form solution for the common mode volume $V_{\mathrm{GI}_{rt}}$, which is a measure of how high the intrinsic coupling loss is when joining two fibers characterized by different profiles (the subscripts t and r refer to transmitting and receiving fibers). Instead, numerical computational methods have to be used [17], which involve determining the intersections (if any) of the differential mode volumes $\rho_t^{-1} dV_{\mathrm{GI}_t}/d(r/\rho_t)$ and $\rho_r^{-1} dV_{\mathrm{GI}_r}/d(r/\rho_r)$ [7].

Since a typical simulation may involve the calculation of 50 000 trials, it is critical to choose an efficient algorithm for numerically solving the aforementioned possible intersections with good precision. The method preferred for general one-dimensional root-finding without available derivatives is usually the Van Wijngaarden–Dekker–Brent Method (or simply Brent's method) [18]. It combines sureness of convergence (once the root of the continuous function has been bracketed) with superlinear convergence and careful handling of roundoff error propagation.

Depending on the number of intersections between the differential mode volumes of the transmitting and receiving fibers, the common mode volume $V_{\mathrm{GI}_{rt}}$ is calculated as indicated in Table VIII (r_{IP1} stands for the radius at which the first intersection between the differential mode volumes $\rho_t^{-1} dV_{\mathrm{GI}_t}/d(r/\rho_t)$ and $\rho_r^{-1} dV_{\mathrm{GI}_r}/d(r/\rho_r)$ occurs; r_{IP2} is the radius of the second intersection, where $r_{\mathrm{IP2}} > r_{\mathrm{IP1}}$) [19].

In contrast, the procedure for calculating the theoretical expressions yielding the common mode volume $V_{\mathrm{MSI}_{rt}}$ of two MSI fibers of any kind that follow the assumptions made in Section II (including the case of two parabolic profile MSI fibers of $N = 100$ layers) is much simpler. We start by solving the fraction of the mode volume V_t of the transmitting fiber transferred to the receiving fiber as

$$\begin{aligned} V_{rt} = 2\pi^2 \Bigg(& \int_0^{\min\{\rho_{1,t},\rho_{1,r}\}} \min\left\{NA_{1,t}^2, NA_{1,r}^2\right\} r dr \\ & + \int_{\min\{\rho_{1,t},\rho_{1,r}\}}^{\max\{\rho_{1,t},\rho_{1,r}\}} \min\left\{NA_{1,p}^2, NA_{2,q}^2\right\} r dr \\ & + \int_{\max\{\rho_{1,t},\rho_{1,r}\}}^{\min\{\rho_{2,t},\rho_{2,r}\}} \min\left\{NA_{2,t}^2, NA_{2,r}^2\right\} r dr \\ & + \int_{\min\{\rho_{2,t},\rho_{2,r}\}}^{\max\{\rho_{2,t},\rho_{2,r}\}} \min\left\{NA_{2,p}^2, NA_{3,q}^2\right\} r dr + \ldots \\ & + \int_{\max\{\rho_{N-1,t},\rho_{N-1,r}\}}^{\min\{\rho_{N,t},\rho_{N,r}\}} \min\left\{NA_{N,t}^2, NA_{N,r}^2\right\} r dr \Bigg) \end{aligned}$$

where the subscripts p and q are set according to

$$\begin{aligned} \text{if } \rho_{i,t} \geqslant \rho_{i,r} &\begin{cases} p = t \\ q = r \end{cases} \\ \text{if } \rho_{i,t} < \rho_{i,r} &\begin{cases} p = r \\ q = t \end{cases} \end{aligned}.$$

We can easily evaluate these integrals and obtain

$$\begin{aligned} V_{rt} = 2\pi^2 \Bigg(& \min\left\{NA_{1,t}^2, NA_{1,r}^2\right\} \frac{\min\left\{\rho_{1,t}^2, \rho_{1,r}^2\right\}}{2} \\ & + \min\left\{NA_{1,p}^2, NA_{2,q}^2\right\} \\ & \times \frac{\max\left\{\rho_{1,t}^2, \rho_{1,r}^2\right\} - \min\left\{\rho_{1,t}^2, \rho_{1,r}^2\right\}}{2} \\ & + \min\left\{NA_{2,t}^2, NA_{2,r}^2\right\} \\ & \times \frac{\min\left\{\rho_{2,t}^2, \rho_{2,r}^2\right\} - \max\left\{\rho_{1,t}^2, \rho_{1,r}^2\right\}}{2} \\ & + \min\left\{NA_{2,p}^2, NA_{3,q}^2\right\} \\ & \times \frac{\max\left\{\rho_{2,t}^2, \rho_{2,r}^2\right\} - \min\left\{\rho_{2,t}^2, \rho_{2,r}^2\right\}}{2} + \ldots \\ & + \min\left\{NA_{N,t}^2, NA_{N,r}^2\right\} \\ & \times \frac{\min\left\{\rho_{N,t}^2, \rho_{N,r}^2\right\} - \max\left\{\rho_{N-1,t}^2, \rho_{N-1,r}^2\right\}}{2} \Bigg) \end{aligned}$$

where the subscripts p and q are set according to the same rules as indicated before.

Last, the equation above can be further reduced to (6) in Section II as

$$\begin{aligned} V_{rt} = 2\pi^2 \sum_{i=1}^{N} \Bigg(& \min\left\{NA_{i-1,p}^2, NA_{i,q}^2\right\} \\ & \times \frac{\max\left\{\rho_{i-1,r}^2, \rho_{i-1,t}^2\right\} - \min\left\{\rho_{i-1,r}^2, \rho_{i-1,t}^2\right\}}{2} \\ & + \min\left\{NA_{i,r}^2, NA_{i,t}^2\right\} \\ & \times \frac{\min\left\{\rho_{i,r}^2, \rho_{i,t}^2\right\} - \max\left\{\rho_{i-1,r}^2, \rho_{i-1,t}^2\right\}}{2} \Bigg) \end{aligned}$$

where $\rho_{0,r} = 0$, $\rho_{0,t} = 0$, $NA_{0,r} = 0$, and $NA_{0,t} = 0$.

The calculations for an MSI fiber have the advantage of not requiring the time-consuming operations associated with bracketing, root finding, and integration. Furthermore, for a GI fiber, the error incurred in making use of the formulae for MSI fibers in Section II instead of those in Table VIII is minimized as the number of layers increases (for instance, for $N = 100$ layers, the percentage error for coupling loss always remains below 0.25%).

ACKNOWLEDGMENT

The authors would like to thank T. Yamamoto of Mitsubishi Rayon Co., Ltd. and Prof. V. Levin of RPC for supplying the MSI-POF samples, and also Prof. H. Poisel of the University of Applied Sciences of Nuremberg for many fruitful discussions.

REFERENCES

[1] K. Ohdoko, T. Ishigure, and Y. Koike, "Propagating mode analysis and design of waveguide parameters of GI POF for very short-reach network use," *IEEE Photon. Technol. Lett.*, vol. 17, no. 1, pp. 79–81, Jan. 2005.

[2] T. Ishigure, K. Makino, S. Tanaka, and Y. Koike, "High-bandwidth graded-index plastic optical fiber enabling power penalty-free gigabit data transmission," *J. Lightw. Technol.*, vol. 21, no. 11, pp. 2923–2930, Nov. 2003.

[3] I. T. Monroy, H. P. A. van de Boom, A. M. J. Koonen, G. D. Khoe, Y. Watanabe, Y. Koike, and T. Ishigure, "Data transmission over polymer optical fibers," *Opt. Fiber Technol.*, vol. 9, no. 3, pp. 159–171, Jul. 2003.

[4] S. Lee, L.-C. Paek, and Y. Chung, "Bandwidth enhancement of plastic optical fiber with multi-step core by thermal diffusion," *Microw. Opt. Technol. Lett.*, vol. 39, no. 2, pp. 129–131, 2003.

[5] K. Irie, Y. Uozu, and T. Yoshimura, "Structure design and analysis of broadband POF," in *Proc. 10th Int. Conf. Plastic Optical Fibers and Applications (POF)*, Amsterdam, The Netherlands, Sep. 2001, pp. 73–79.

[6] G. Aldabaldetreku, G. Durana, J. Zubia, J. Arrue, F. Jiménez, and J. Mateo, "Analysis of intrinsic coupling loss in multi-step index optical fibres," *Opt. Express*, vol. 13, no. 9, pp. 3283–3295, May 2005. [Online]. Available: http://www.opticsexpress.org/abstract.cfm?URI=OPEX-13-9-3283

[7] F. L. Thiel and D. H. Davis, "Contributions of optical-waveguide manufacturing variations to joint loss," *Electron. Lett.*, vol. 12, no. 13, pp. 340–341, 1976.

[8] F. L. Thiel and R. M. Hawk, "Optical waveguide cable connection," *Appl. Opt.*, vol. 15, no. 11, pp. 2785–2791, Nov. 1976.

[9] J. Zubia, G. Aldabaldetreku, G. Durana, J. Arrue, H. Poisel, and C. A. Bunge, "Geometric optics analysis of multi-step index optical fibers," *Fiber Integr. Opt.*, vol. 23, no. 2/3, pp. 121–156, Mar.–Jun. 2004.

[10] Mitsubishi Rayon Co., Ltd. (2006). *Eska Miu*. Tokyo, Japan: Optical Fiber Dept. [Online]. Available: http://www.pofeska.com

[11] V. Levin, T. Baskakova, Z. Lavrova, A. Zubkov, H. Poisel, and K. Klein, "Production of multilayer polymer optical fibers," in *Proc. 8th Int. Conf. Plastic Optical Fibers and Applications (POF)*, Chiba, Japan, Jul. 1999, pp. 98–101.

[12] D. Marcuse, *Principles of Optical Fiber Measurements*. London, U.K.: Academic, 1981, ch. 4.
[13] Japanese Standards Association, "Test methods for structural parameters of all plastic multimode optical fibers," JIS, Tokyo, Japan, Tech. Rep. JIS C 6862, 1990.
[14] A. W. Snyder and J. D. Love, *Optical Waveguide Theory*. London, U.K.: Chapman & Hall, 1983.
[15] A. Ankiewicz and C. Pask, "The effects of source configuration on bandwidth and loss measurements in optical fibres," *Opt. Quantum Electron.*, vol. 15, no. 6, pp. 463–470, 1983.
[16] D. Gloge and E. A. J. Marcatili, "Multimode theory of graded-core fibers," *Bell Syst. Tech. J.*, vol. 52, no. 9, pp. 1563–1578, 1973.
[17] W. H. Press, B. P. Flannery, S. A. Teukolsky, and W. T. Vetterling, *Numerical Recipes in C: The Art of Scientific Computing*. Cambridge, U.K.: Cambridge Univ. Press, 2002.
[18] R. P. Brent, *Algorithms for Minimization Without Derivatives*. Englewood Cliffs, NJ: Prentice-Hall, 1973.
[19] S. C. Mettler, "A general characterization of splice loss for multimode optical fibers," *Bell Syst. Tech. J.*, vol. 58, no. 10, pp. 2163–2182, 1979.

G. Aldabaldetreku received the M.Sc. degree in telecommunications engineering from the University of the Basque Country, Bilbao, Spain, in 2000, where he is currently working toward the Ph.D. degree in theoretical analysis of multistep index (MSI) fibers.

He has been researching polymer optical fibers at the School of Engineering, University of the Basque Country, for nearly five years. In 2002, he became an Assistant Lecturer at the School of Engineering of the same university.

G. Durana received the M.Sc. degree in solid-state physics from the University of the Basque Country, Bilbao, Spain, in 1999 and is currently working toward the Ph.D. degree in the study of light polarization properties in polymer optical fibers (POFs).

He is currently a Lecturer and a Researcher at the Telecommunications Department, School of Engineering, University of the Basque Country.

J. Zubia received the M.Sc. degree in solid-state physics in 1988 and the Ph.D. degree in physics in 1993, both from the University of the Basque Country, Bilbao, Spain. His Ph.D. work focused on optical properties of ferroelectric liquid crystals.

He is currently a Full Professor at the Telecommunications Engineering School, University of the Basque Country. He has more than ten years of experience doing basic research in the field of polymer optical fibers. At present, he is involved in research projects in collaboration with universities and companies from Spain and other countries in the field of polymer optical fibers, fiber-optic sensors, and liquid crystals.

Prof. Zubia won a special award for Best Thesis in 1995.

J. Arrue received the M.Sc. degree in electronic physics in 1990, completed a 12-month postgraduate course in electronics in 1991 and a 12-month postgraduate course in telecommunications in 1992, and received the Ph.D. degree in optical fibers in 2001, all from the University of the Basque Country, Bilbao, Spain.

He is currently a Professor at the Telecommunications Engineering School of Bilbao, University of the Basque Country. He is also involved in international research projects with other universities and companies.

Dr. Arrue won a special award for his thesis and an European acknowledgement of the Ph.D. degree.